Scaling of postinjection-induced seismicity –
Understanding of non-linear back fronts

L. Johann*, C. Dinske, S. A. Shapiro

Freie Universität Berlin, FR Geophysik

Schatzalp Workshop 2017

Johann, L., Dinske, C., and Shapiro, S. A. (2016). Scaling of seismicity induced by nonlinear fluid-rock interaction after an injection stop. *Journal Geophysical Research: Solid Earth*, **121**:1–21.

MOTIVATION

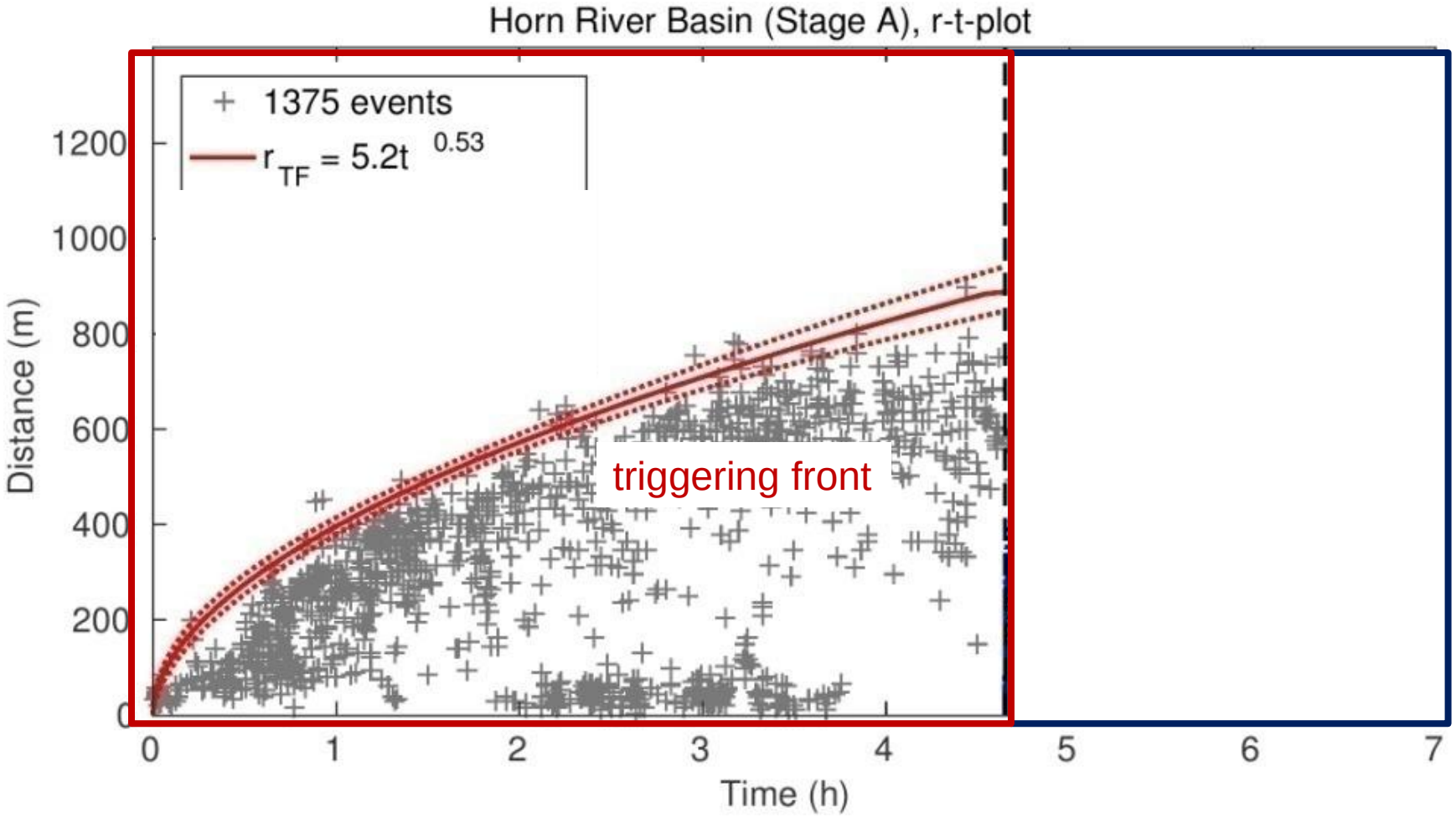
Horn River Basin (Stage A), r-t-plot
1375 events
$r_{TF} = 5.2t^{0.53}$
triggering front
Distance (m)
Time (h)
0
200
400
600
800
1000
1200
0
1
2
3
4
5
6
7

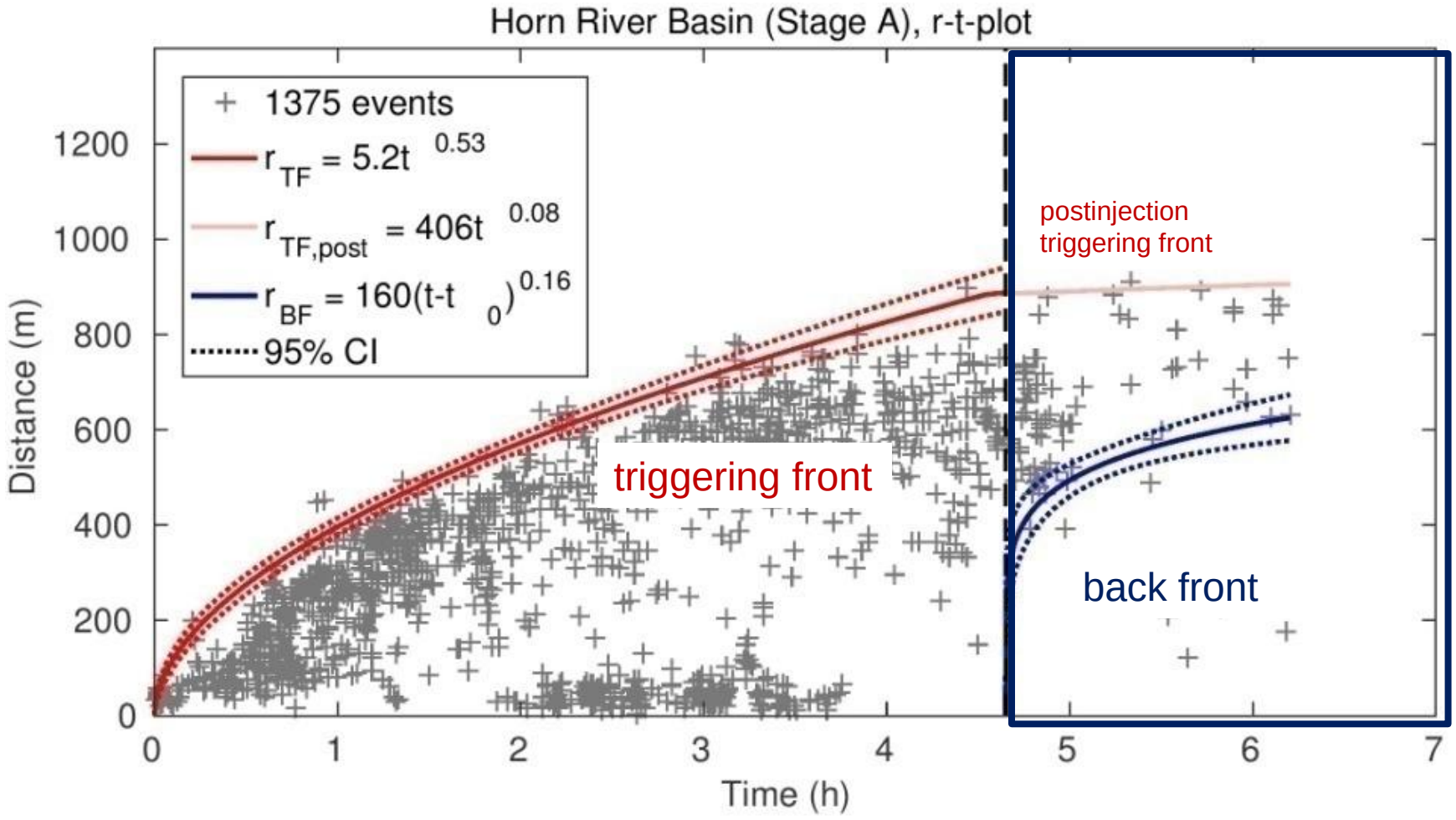
Horn River Basin (Stage A), r-t-plot
1375 events
$r_{TF} = 5.2t^{0.53}$
$r_{TF,post} = 406t^{0.08}$
$r_{BF} = 160(t-t_0)^{0.16}$
95% CI
Distance (m)
Time (h)
0
200
400
600
800
1000
1200
0
1
2
3
4
5
6
7
triggering front
postinjection
triggering front
back front

Mathematical background to understand our theoretical approach

NON-LINEAR PORE-FLUID PRESSURE DIFFUSION

General **equation of diffusion**

$$\frac{\partial p}{\partial t} = \nabla\left(D(p)\nabla p\right)$$

for a *d*-dimensional, hydraulically isotropic and homogeneous medium.

Power law dependence of hydraulic diffusivity on pressure
(Shapiro and Dinske, 2009)

$$D(p) = (n+1)D_0 p^n$$

Scaling of coinjection-induced triggering front

Shapiro& Dinske (2009)

$$r_{tf} \propto \left(D_0 Q_0{}^{n} t^{n(i+1)+1} \right)^{(dn+2)^{-1}}$$

Q_0 : normalization parameter, defining the fluid injection rate $Q_i(t)$

i: defines the injection rate

i = -1: delta-like

i = 0: constant

d: dimension of the diffusion

d = 1, 2, 3

Scaling of postinjection-induced fronts

For a $\delta(t)$-like impulse of fluid injection and $t >> t_0$

$$r \propto t^{(dn+2)^{-1}}$$

Valid for back front and triggering front

Validation of the scaling law

NUMERICAL MODELLING

Numerical results: Pressure relaxation

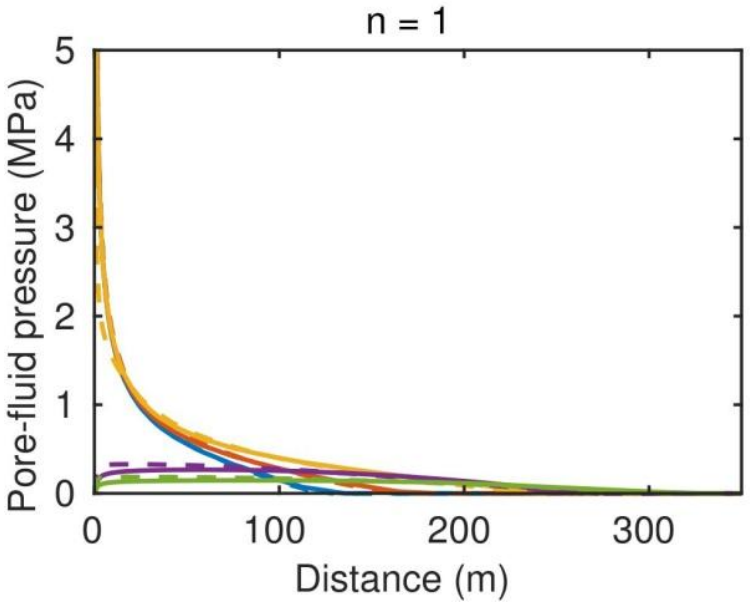

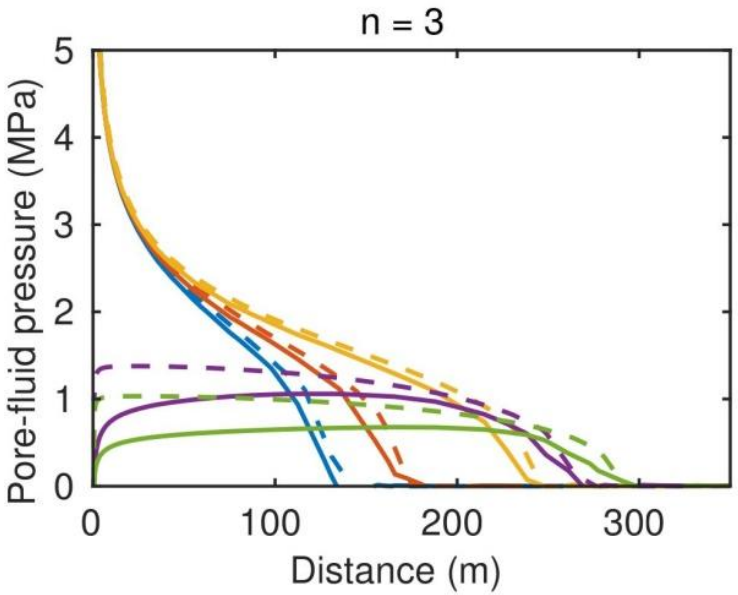

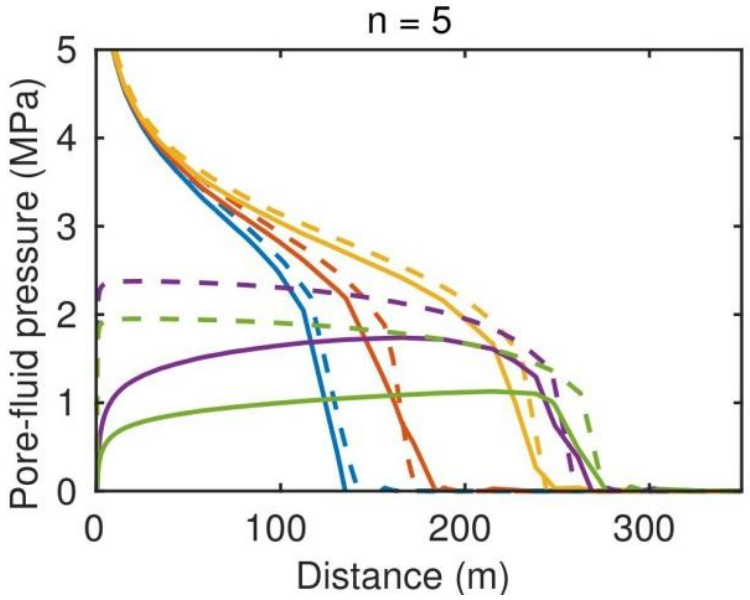

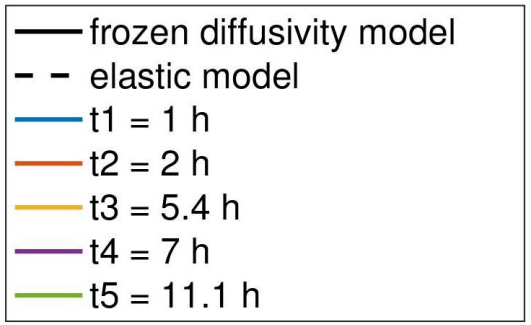

Synthetic seismicity

$$p(x,y,z,t) > C(x,y,z)$$

C(x,y,z): Pressure necessary for activation of critically stressed, favorably oriented preexisting fractures

Numerical results II : *r-t*-plots

1) Linear diffusion fronts (- -)
2) Power law fits (-)
3) Confidence interval, CI (:)

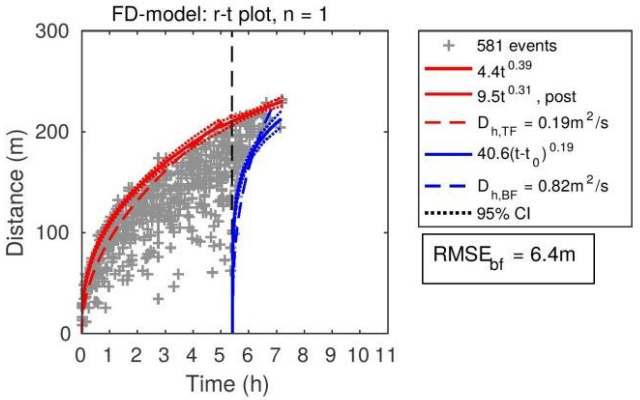

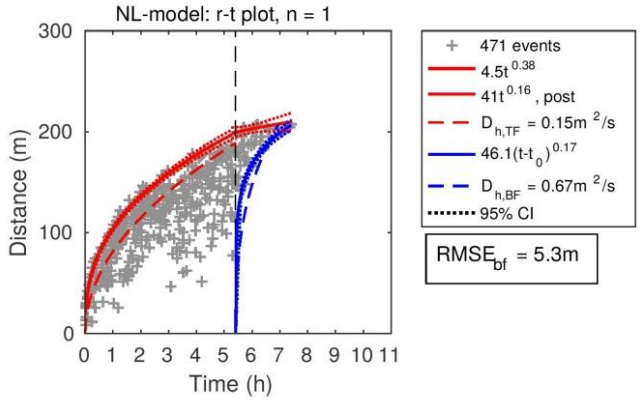

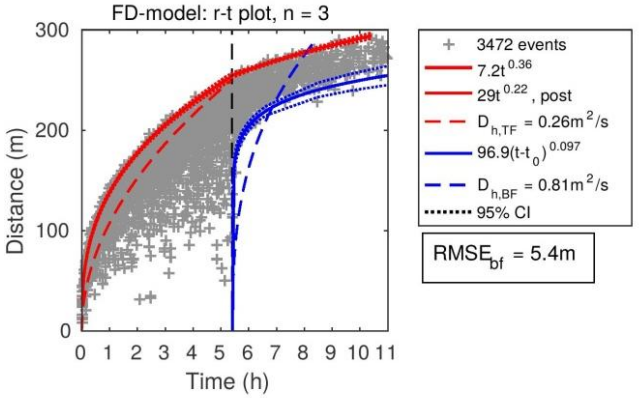

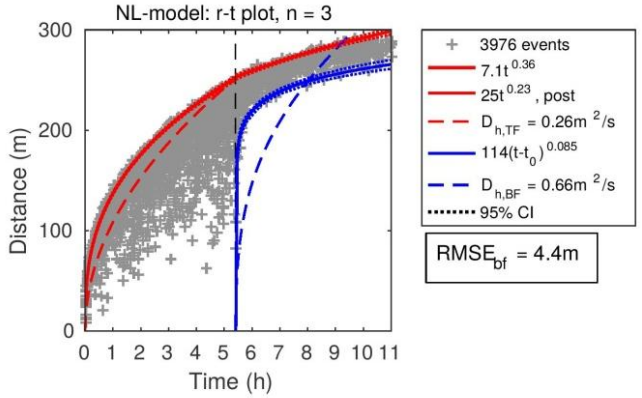

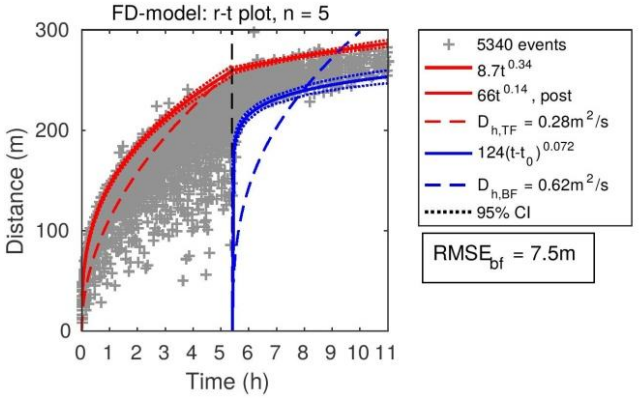

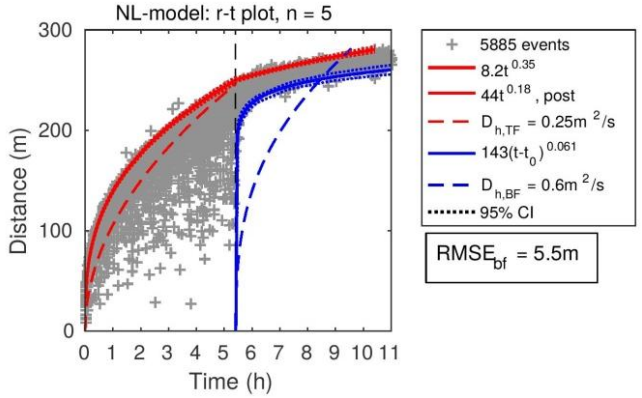

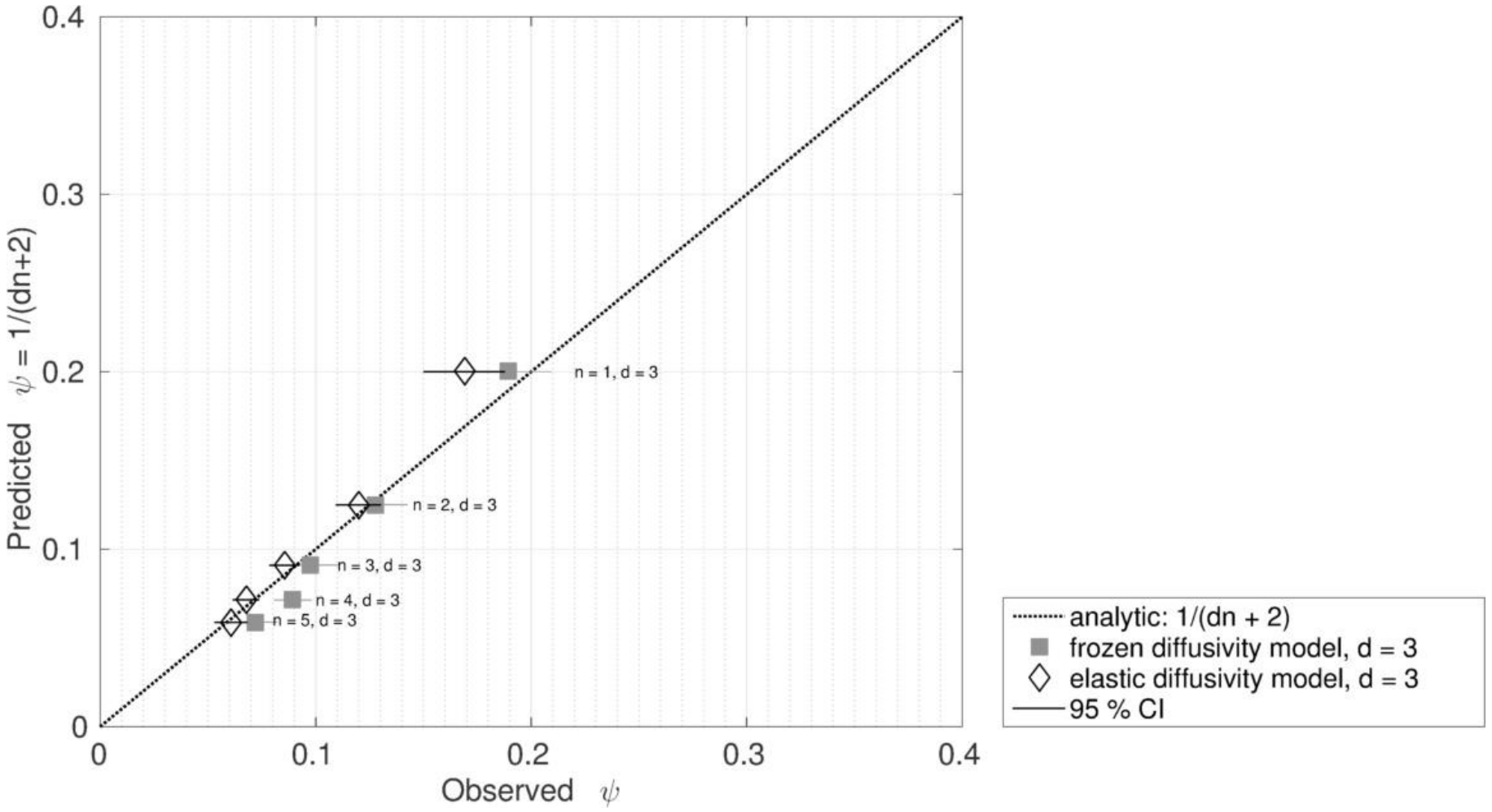
0.4
0.3
0.2
0.1
0
Predicted $\psi = 1/(dn+2)$
0
0.1
0.2
0.3
0.4
Observed ψ
n = 1, d = 3
n = 2, d = 3
n = 3, d = 3
n = 4, d = 3
n = 5, d = 3
analytic: 1/(dn + 2)
frozen diffusivity model, d = 3
elastic diffusivity model, d = 3
95 % CI

Benefit from scaling law

APPLICATION TO REAL DATA

Hydraulic fracturing and EGS data

(a)

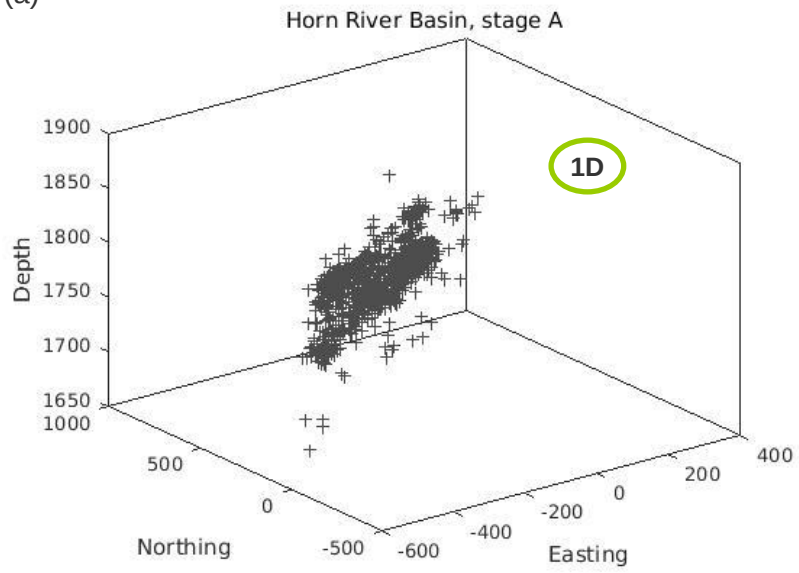

(b)

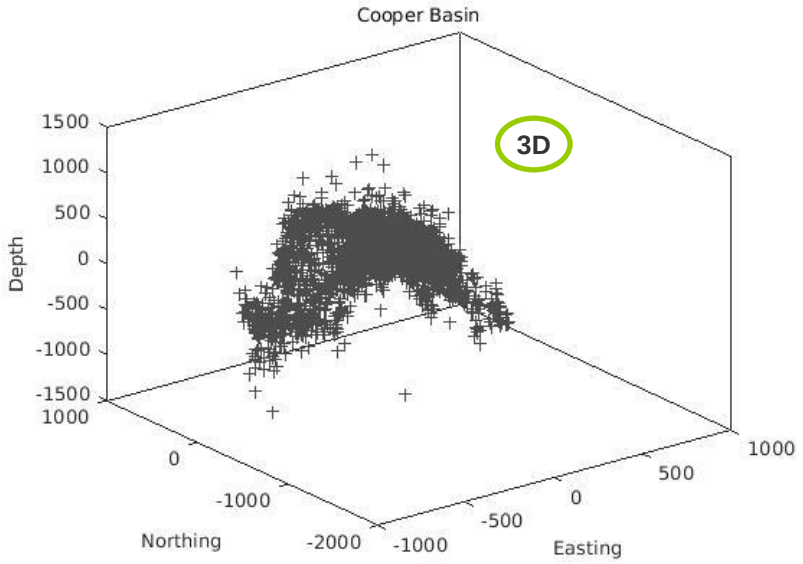

(a) Data provided by one sponsor of the PHASE consortium
(b) Data are courtesy of H. Kaieda

Hydraulic fracturing and EGS data

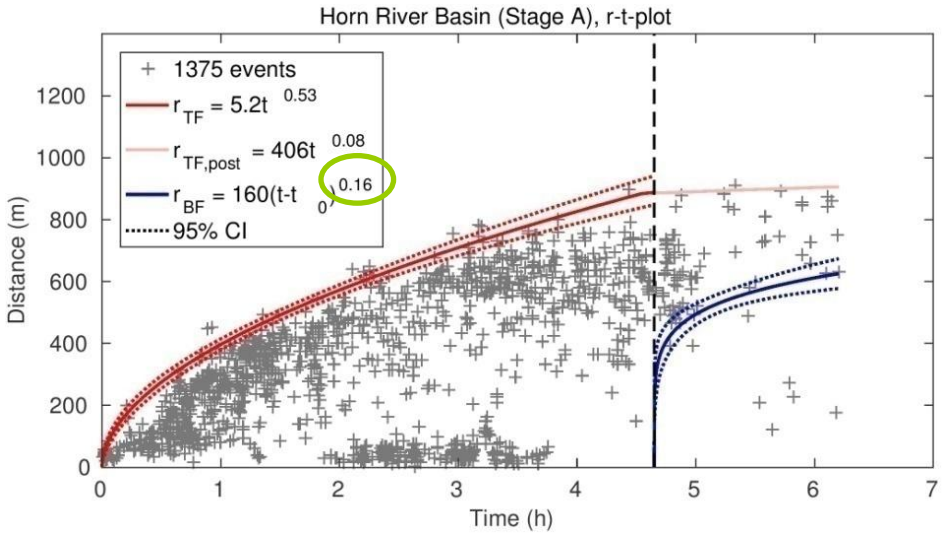

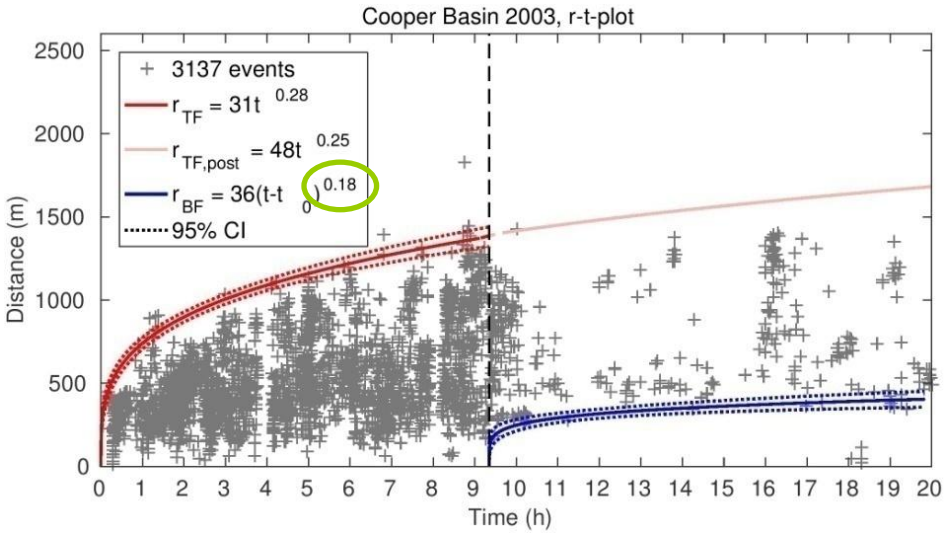

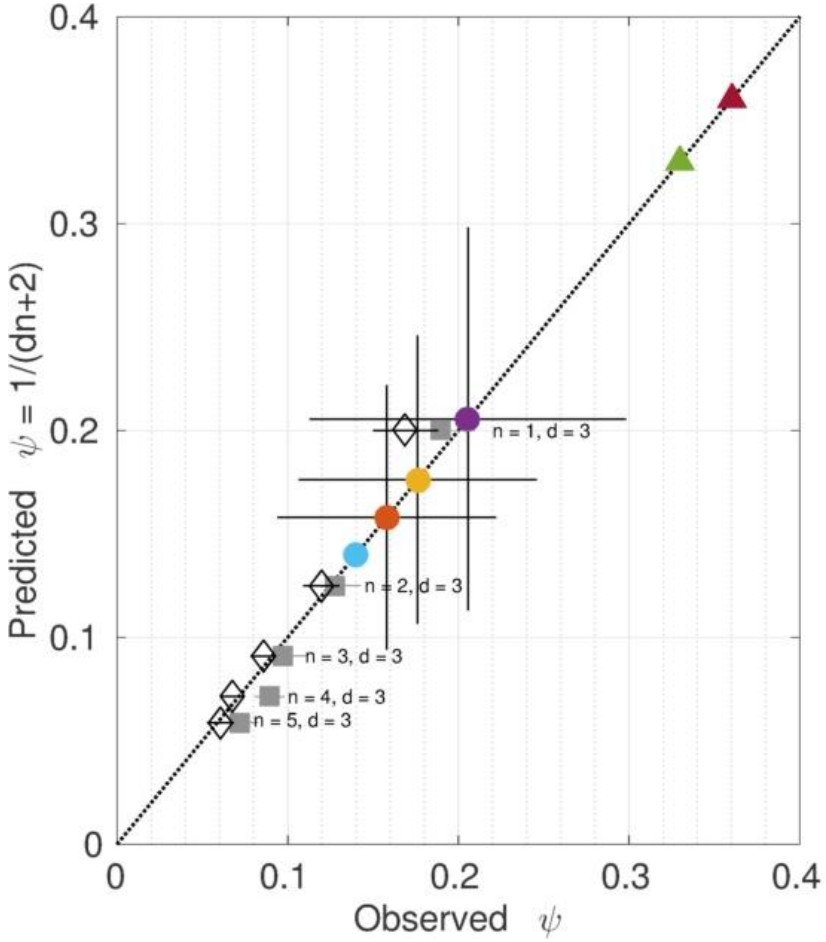

analytic: 1/(dn + 2)
frozen diffusivity model, d = 3
elastic diffusivity model, d = 3
Cooper Basin 2003, 0.69 < n < 2.5, d = 3
Horn River Basin, stage A, 2.5 < n < 8.6, d = 1
Basel 2006, 0.45 < n < 2.3, d = 3
Montney Shale (SpectraSeis), Lower Well, n = 5.1, d = 1
Ogachi (Hummel and Shapiro, 2015), n = 0.26, d = 3
Fenton Hill (Hummel and Shapiro, 2015), n = 0.34, d = 3
95 % CI

CONCLUSIONS

Novel scaling relations for **postinjection-induced** seismicity:

Spatio-temporal evolution is controlled by **dimension** of growth of seismic cloud *d* and **non-linearity** *n* of pore-fluid pressure diffusion

→ If two parameters are known (e.g. Ψ *or* χ and *d*), estimates of the third (e.g. *n*) can be obtained

Restrictions

Assumption of purely **non-linear diffusion** as the seismicity controlling process, which is one end-member case of **poroelastic coupling**

THANK YOU

Acknowledgements

We thank the sponsors of the PHASE consortium for supporting the research presented here

References

Hummel, N. and S. A. Shapiro (2016), Back front of seismicity induced by non-linear pore pressure diffusion, *Geophys. Pros., 64(1*), 170-191.

Hummel, N. and S. A. Shapiro (2013), Nonlinear diffusion-based interpretation of induced microseismicity: A Barnett Shale hydraulic fracturing case study, *Geophysics, 78*, B211-B226.

Johann, L., Dinske, C., and Shapiro, S. A. (2016). Scaling of seismicity induced by nonlinear fluid-rock interaction after an injection stop. Journal Geophysical Research: Solid Earth, 121:1–21.

Rothert, E. and S. A. Shapiro (2003), Microseismic monitoring of borehole fluid-injections: Data modeling and inversion for hydraulic properties of rocks., *Geophysics, 68*, 685-689.

Shapiro, S. A. and C. Dinske (2009), Scaling of seismicity induced by nonlinear fluid-rock interaction, *JGR, 114,* 14pp.

Shapiro et al. (2002), Characterization of fluid transport properties of reservoirs using induced microseismicity, *Geophysics, 67*, 212-220.

Shapiro et al. (1999), Large-scale in situ permeability tensor of rocks from induced microseismicty, *Geophys. J. Int., 137*, 207-213.

Shapiro et al. (1997), Estimating the permeability from fluid-injection induced seismic emission at the KTB site, *Geophys. J. Int., 131*, F15-F18.

APPENDIX

Microseismicity during fluid-injections

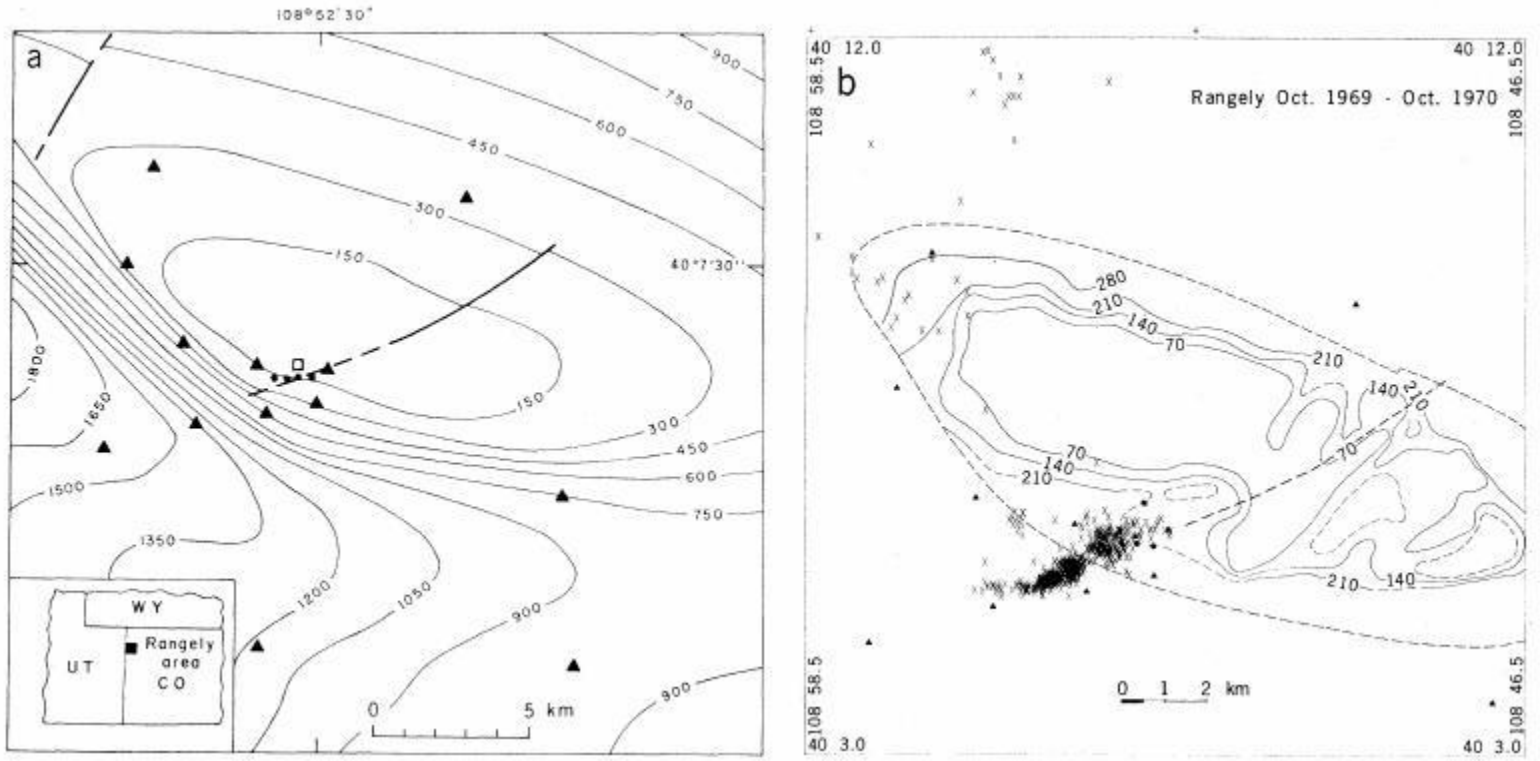

Figure by Raleigh et al. (1976)

(a) Structure contour map of Rangely, Colorado
(-) depth below sealevel
(•) wells for fluid pressure
(Δ) seism. Stations

(b) (x) Seismicity 10/1969 - 11/1970
(-) bottom-hole pressure (09/1969)

Microseismicity during fluid-injections

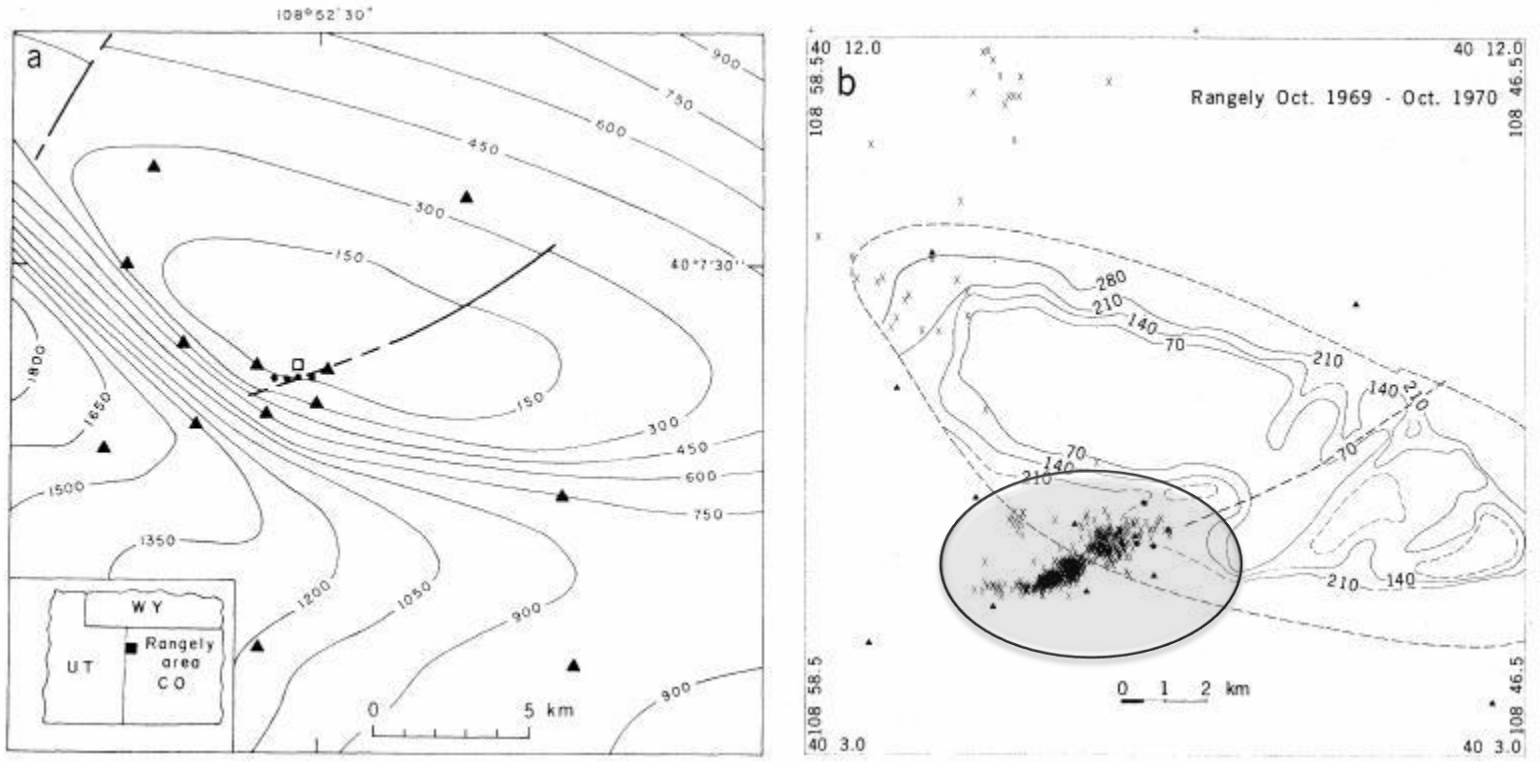

Figure by Raleigh et al. (1976)

(a) Structure contour map of Rangely, Colorado
(-) depth below sealevel
(•) wells for fluid pressure
(Δ) seism. Stations

(b) (x) Seismicity 10/1969 - 11/1970
(-) bottom-hole pressure (09/1969)

Spatio-temporal analysis of seismic events for

1) reservoir characterization (Shapiro 1997, 1999, 2002)
2) general understanding of physical processes linked to seismicity

FE Model

based on Barnett Shale hydraulic fracturing (Hummel and Shapiro, 2013)

Parameter

$D(p) = (n+1)D_0\, p^n$

n = 1,2,..5

D_0 for n such that $p(r,t_0)$ = 0 Pa at r = 250 m

Modeling time

t = [0, 40000 s], Δt = 60 s

t_0 = 19500 s

Postinjection diffusivity

Elastic behavior vs. frozen diffusivity

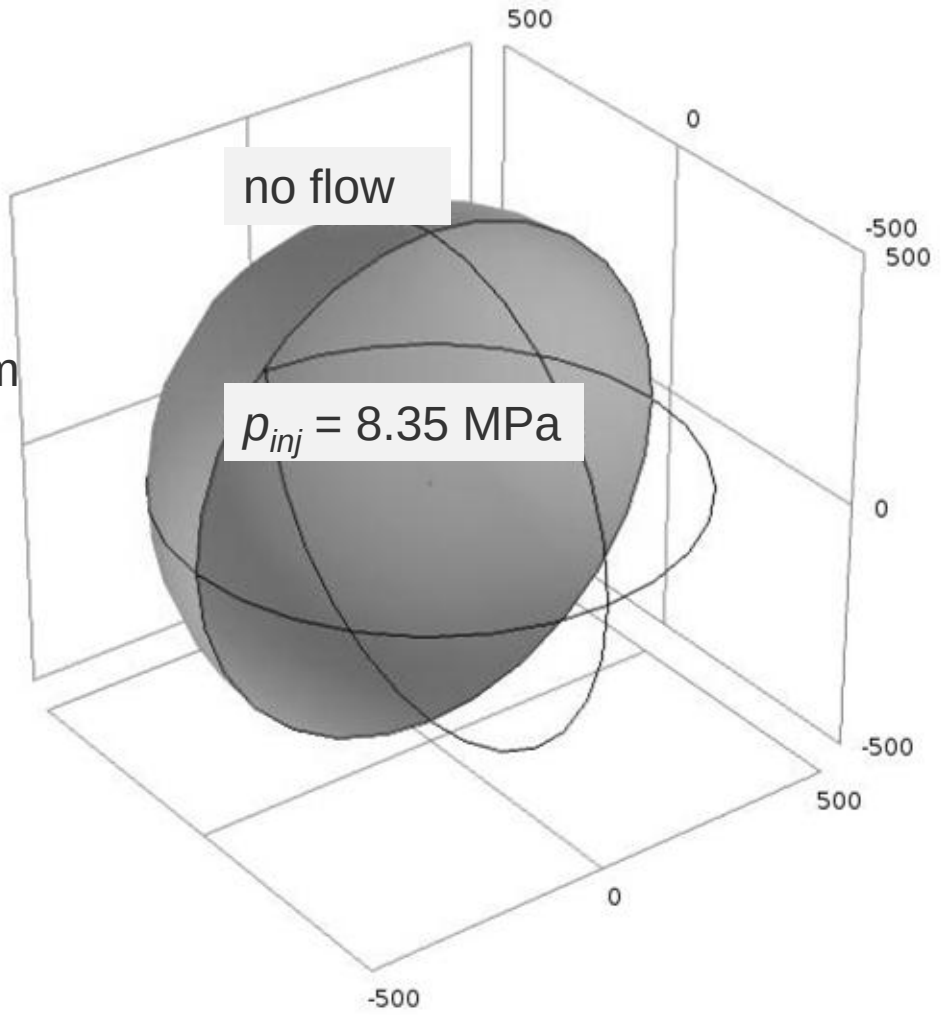

Elastic Diffusivity

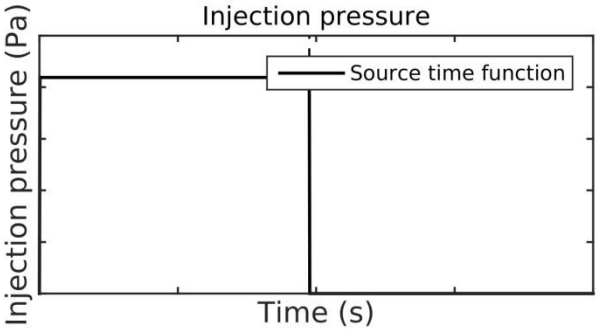

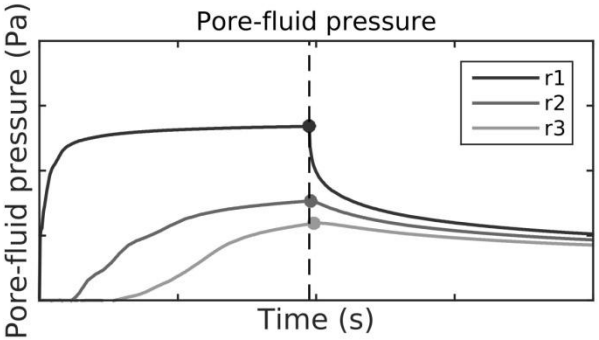

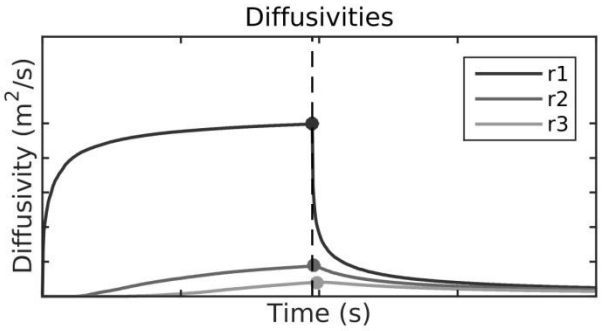

Frozen Diffusivity

(Hummel and Shapiro, 2016)

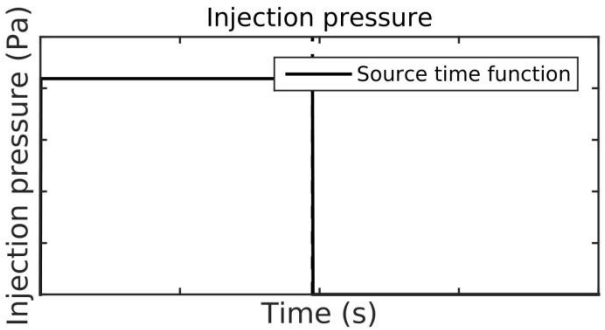

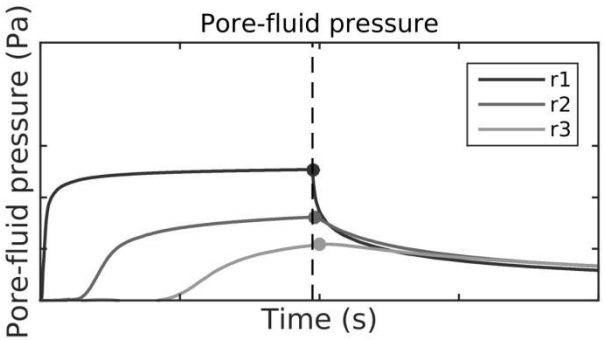

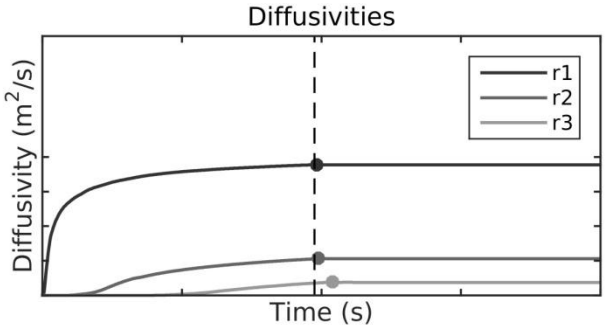

Quantification of *r-t*-plots

Power law fits to the co-injection triggering front

$$r_{tf} = At^{\chi}$$

and to the back front of seismicity

$$r_{bf} = B(t - t_0)^{\psi}$$

For 3D power law diffusion (Hummel & Shapiro, 2012, 2016)

χ = 0.5: linear diffusion, χ = 0.33: non-linear diffusion

ψ = 0.33: linear diffusion, ψ < 0.33: non-linear diffusion

Shapiro & Dinske (2009) for the coinjection triggering front:

Diffusion equation for radial symm. hydraulically homogeneous & isotropic medium:

$$\frac{\partial r^{d-1} p}{\partial t} = D_0 \frac{\partial}{\partial r} r^{d-1} \frac{\partial}{\partial r} p^{n+1}$$

Fluid injection rate

$$Q_i(t) = S(i+1) A_d Q_0 t^i$$

Mass conservation for $Q_i(t)$:

$$\int_0^\infty r^{d-1} p(t,r)\, \mathrm{d}r \;=\; Q_0 t^{i+1}\,.$$

Dimensionless variable Θ from dimensional analysis

$$\theta = r\left(D_0 Q_0^n t^{n(i+1)+1}\right)^{\frac{-1}{(dn+2)}}\,.$$

S: storage coefficient (1/Pa)

A_d: 4 , 2h, 2Ar for 3D, 2D, 1D

Q_0: normalizing coefficient

A combination of the quantities in equation 11 yields the dimension of pressure $p = [P]$:

$$\left(\frac{Q_0^2}{D_0^d t^{(d-2i-2)}}\right)^{\frac{1}{(dn+2)}}$$

Following the Π-theorem as defined in *Barenblatt* [1996], a description of pressure can then be formulated as follows:

$$p(t,r) = \left(\frac{Q_0^2}{D_0^d t^{(d-2i-2)}}\right)^{1/(dn+2)} \Phi(\theta)\,.$$

Here $\Phi(\theta)$ is a dimensionless function found by substituting (5) and (13) into (8) and (10) and applying the boundary condition $p = 0\,\mathrm{Pa}$ for $t < 0\,\mathrm{s}$ [see equations (4.36) - (4.37) in *Shapiro*, 2015].

Further, rearranging (11) yields a general proportionality for the triggering front

$$r_{tf} \propto (D_0 Q_0^n t^{n(i+1)+1})^{\frac{1}{(dn+2)}}\,.$$

Additionally, *Hummel and Shapiro* [2012] investigate triggering front signatures for a constant injection pressure source ($i = 0$). Their results show that p in equation 6 is very well described by $p = (n+1)/(dn+2)$, what is in agreement with equation 14.

Under the above mentioned assumptions of $i = -1$ and a point-like (in d-dimensional space) injection source located at $r = 0\,\mathrm{m}$, equation 13 can be written as:

$$p(t,0) = \left(\frac{Q_0^2}{D_0^d t^d}\right)^{1/(dn+2)} \Phi(0)\,, \tag{15}$$

where $\Phi(0)$ is a constant. Using the expression for the pressure distribution $p(t,0)$, equation 13 can be reformulated, yielding the pressure distribution at distances r smaller than the triggering front r_{tf} [*Shapiro and Dinske*, 2009; *Shapiro*, 2015]:

$$p(t,r) = p(t,0)\left(1 - \frac{r^2}{r_{tf}^2}\right)^{1/n}. \tag{16}$$

Please note that $p = 0$ if $r > r_{tf}$.

Assuming that events are only induced for increasing pore-fluid pressure, the condition for the back front is given by the vanishing partial time derivative $\frac{\partial p(t,r)}{\partial t}$. Using equation 16 for computing this derivative, we get:

$$\frac{\partial p(t,0)}{\partial t}\left(1 - \frac{r^2}{r_{tf}^2}\right)^{1/n} + \frac{2}{n}p(t,0)\left(1 - \frac{r^2}{r_{tf}^2}\right)^{(1-n)/n}\frac{r^2}{r_{tf}^3}\frac{\partial r_{tf}}{\partial t} = 0\,. \tag{17}$$

The partial time derivative of the pressure distribution $p(t,0)$ (equation 15) is given by:

$$\frac{\partial p(t,0)}{\partial t} = t^{d/(dn+2)}\frac{1}{t}p(t,0) = \frac{-d}{dn+2}t^{-1}p(t,0)\,. \tag{18}$$

$$0 = \frac{-d}{dn+2} t^{-1} + \frac{2}{n} \left(1 - \frac{r^2}{r_{tf}^2}\right)^{-1} \frac{r^2}{r_{tf}^3} \frac{\partial r_{tf}}{\partial t} .$$

Using $i = -1$ in equation 14, we get:

$$r_{tf} \propto (Q_0^n D_0 t)^{1/(dn+2)} . \tag{20}$$

The function $\partial r_{tf}(t)/\partial t$ in equation 19 can be found from equation 20. It is given by:

$$\frac{\partial r_{tf}}{\partial t} \propto \frac{1}{dn+2} (D_0 Q_0^n)^{1/dn+2} t^{-(dn+1)/(dn+2)} . \tag{21}$$

Subsequently, the combination of equations 20 and 21 yields (note that a proportionality constant in these equations is eliminated in this way):

$$\frac{1}{r_{tf}} \frac{\partial r_{tf}}{\partial t} = \frac{1}{dn+2} t^{-1} . \tag{22}$$

Substituting this into equation 19 gives the following result:

$$dn = (2+dn) \frac{r^2}{r_{tf}^2} , \tag{23}$$

where r is a function of time, describing the back front distance from the source, r_{bf}. Thus,

$$r_{bf}(t) = r_{tf}(t) \left(\frac{dn}{2+dn} \right)^{(1/2)} \tag{24}$$

Table 1. Values of the Exponent ψ (Equation (7)) Obtained From Synthetic Data and Real Data Examples From Literature[a]

FD Model	Observed ψ	Predicted $1/(dn+2)$	ED Model	Observed ψ	Predicted $1/(dn+2)$
$n=1$	$0.17 < 0.19 < 0.21$	0.20	$n=1$	$0.15 < 0.17 < 0.19$	0.20
$n=2$	$0.11 < 0.13 < 0.14$	0.125	$n=2$	$0.11 < 0.12 < 0.13$	0.125
$n=3$	$0.085 < 0.097 < 0.11$	0.091	$n=3$	$0.079 < 0.086 < 0.092$	0.091
$n=4$	$0.081 < 0.089 < 0.098$	0.071	$n=4$	$0.062 < 0.068 < 0.073$	0.071
$n=5$	$0.063 < 0.072 < 0.082$	0.059	$n=5$	$0.053 < 0.061 < 0.068$	0.059
Hydraulic fracturing data				observed ψ	estimated n
Horn River Basin (relocated events by A. Reshetnikov)				$0.095 < 0.16 < 0.22$	$2.5 < 4.3 < 8.6$
Montney Shale, lower (*r-t* by *Birkelo et al.* [2012])				0.14	5.1
EGS data				observed ψ	estimated n
Basel 2006				$0.11 < 0.21 < 0.30$	$0.45 < 0.95 < 2.3$
Cooper Basin 2003				$0.11 < 0.18 < 0.25$	$0.69 < 1.2 < 2.5$
Fenton Hill (ψ by *Hummel and Shapiro* [2016])				0.33	0.34
Ogachi (ψ by *Hummel and Shapiro* [2016])				0.36	0.26

[a]For synthetic data, also predicted values for $1/(dn+2)$ (equation (25)) are given for the frozen diffusivity model (FD model) and the reversible elastic diffusivity model (ED model). For real data, equation (25) was applied, yielding estimates of the nonlinearity n within 95% confidence intervals. Values of observed ψ and predicted $1/(dn+2)$ are plotted in Figure 5.

From Johann et al. (2016), JGR

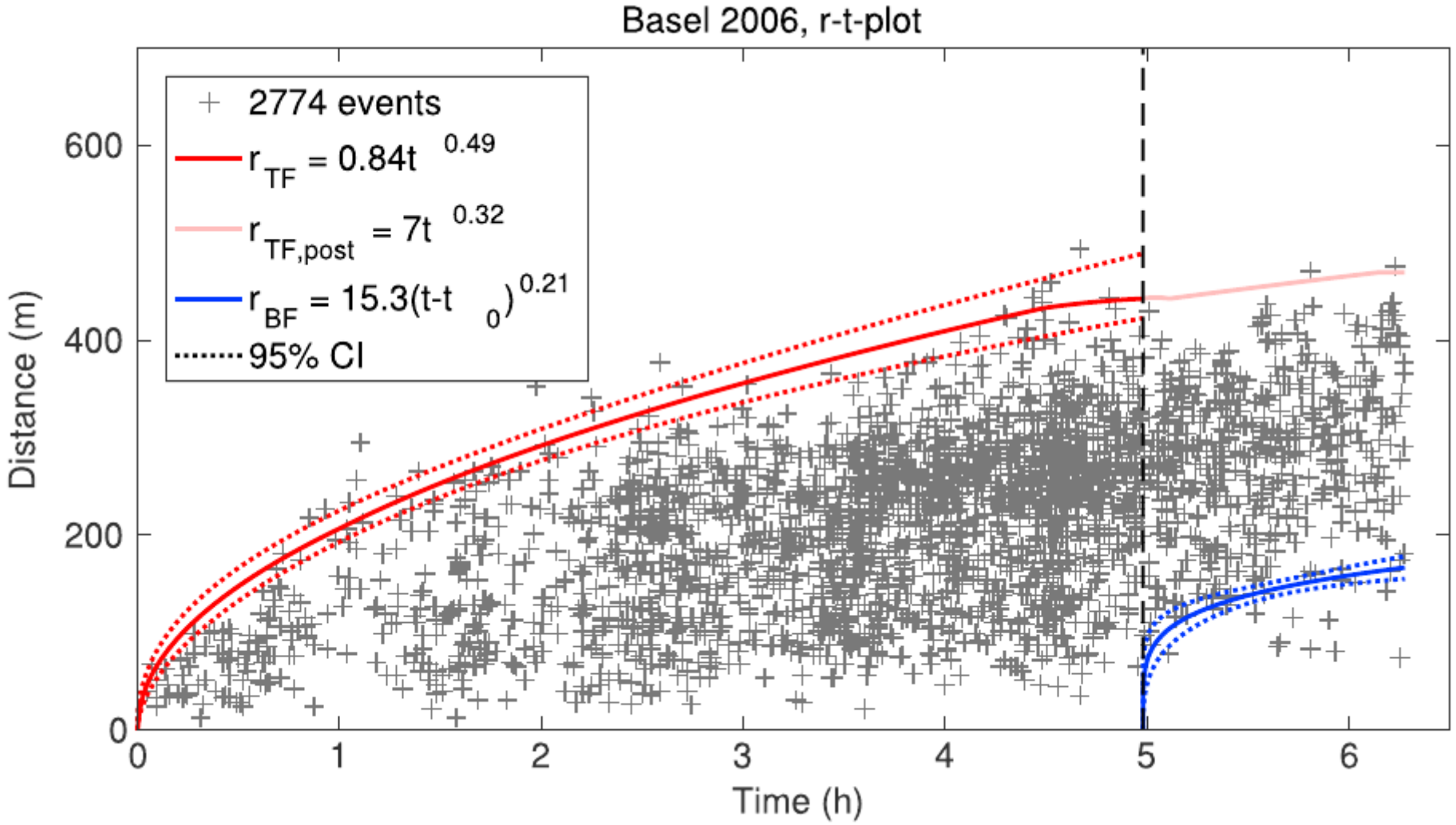
Basel 2006, r-t-plot
2774 events
$r_{TF} = 0.84t^{0.49}$
$r_{TF,post} = 7t^{0.32}$
$r_{BF} = 15.3(t-t_0)^{0.21}$
95% CI
Distance (m)
Time (h)
0
200
400
600
0
1
2
3
4
5
6

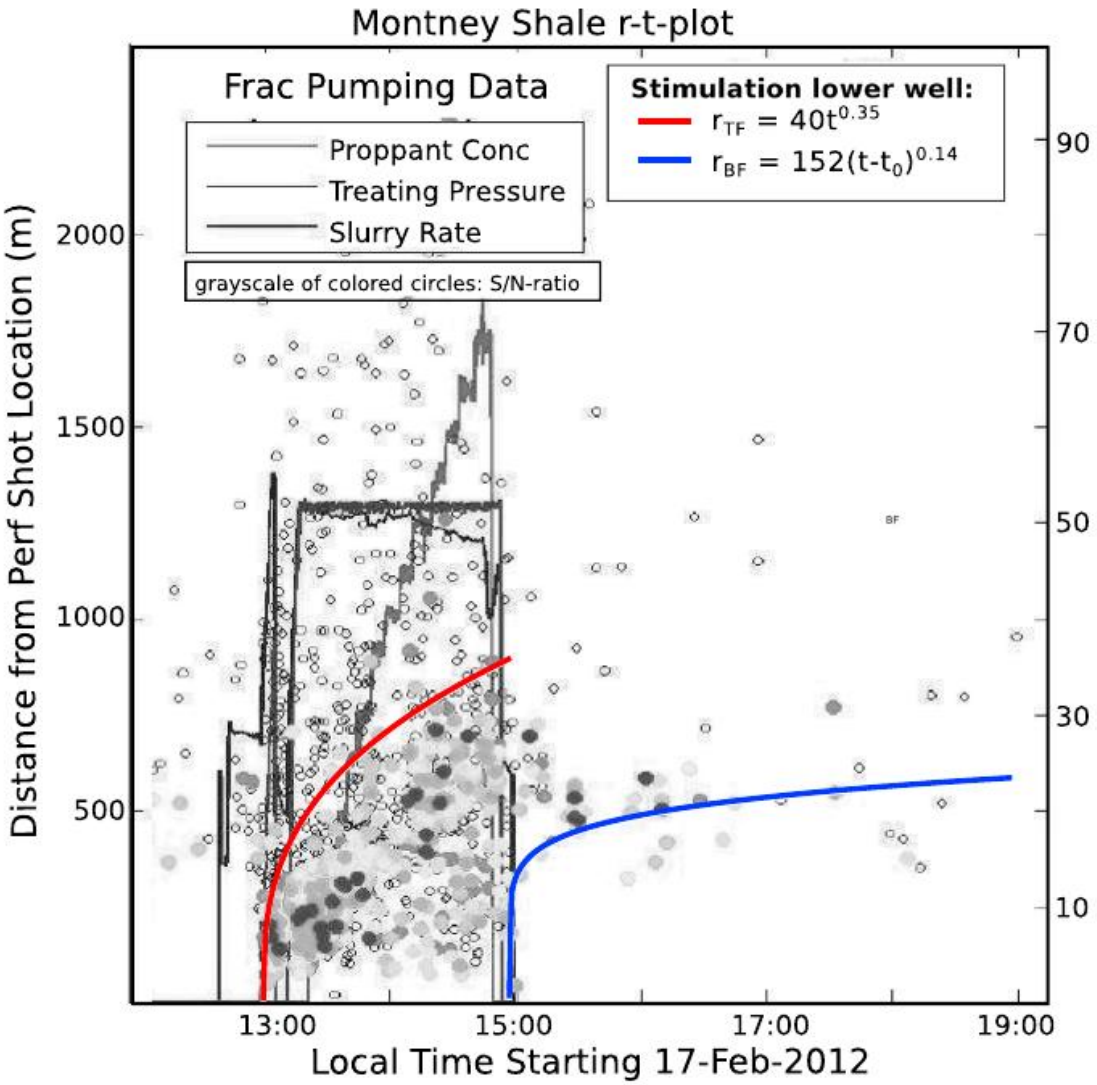
Montney Shale r-t-plot
Frac Pumping Data
Proppant Conc
Treating Pressure
Slurry Rate
grayscale of colored circles: S/N-ratio
Stimulation lower well:
$r_{TF} = 40t^{0.35}$
$r_{BF} = 152(t-t_0)^{0.14}$
Distance from Perf Shot Location (m)
2000
1500
1000
500
90
70
50
30
10
13:00
15:00
17:00
19:00
Local Time Starting 17-Feb-2012